SPEED-FLOW RELATIONSHIP AND CAPACITY FOR EXPRESSWAYS IN BRAZIL

Gustavo Riente de Andrade
Ph.D. Candidate
Universidade de São Paulo
São Carlos School of Engineering
Department of Transportation Engineering
400 Trabalhador São-carlense Avenue
São Carlos, SP, Brazil – 13566-590
Phone: (+55-16) 3373-9596
Fax: (+55-16) 3373-9602
E-mail: guriente@hotmail.com

José Reynaldo Setti (*)
Professor of Civil Engineering
Universidade de São Paulo
São Carlos School of Engineering
Department of Transportation Engineering
400 Trabalhador São-carlense Avenue
São Carlos, SP, Brazil – 13566-590
Phone: (+55-16) 3373-9596
Fax: (+55-16) 3373-9602
E-mail: jrasetti@usp.br

(*) Corresponding author

Text:	4,646 words
Figures:	6 × 250 = 1,500 words
Tables:	2 × 250 = 500 words
References:	28 references = 500 words
Total:	7,146 words

Paper submitted on July 30, 2013
Revised version submitted on November 14, 2013

ABSTRACT

This paper presents the development of a speed-flow model for expressways in Brazil, similar to the one used in the HCM 2010. The model was developed using a sample of 788,122 observations, collected at 24 stations on four expressways in the state of São Paulo. The data analysis showed that, as proposed by the HCM 2010, there is range of flows in which the average speed of the passenger cars remains constant and equal to the free flow speed. It was also found that the classification scheme used by the HCM 2010, based on control of access (freeways vs. multilane highways), is not adequate for expressways in the state of São Paulo. A new scheme, which divides expressways into urban and rural sections, is proposed. For these highway classes, representative values for the capacity were found, and speed-flow relationships were calibrated.

1. INTRODUCTION

The Highway Capacity Manual (HCM) has been widely adopted outside the U.S.A. as the standard to estimate level of service. In Brazil, it has been adopted to assess both existing operational conditions and the benefits of proposed highway improvements (*1*). However, many highway administrators, practitioners and researchers have been advocating the adaptation of HCM procedures to local road and traffic characteristics (*1, 2, 3, 4, 5, 6*). The main aspects to be adapted are speed-flow relationships, including base conditions and capacity, and passenger-car equivalents for trucks (*5*). While the latter have already been studied (*2, 7*), the calibration of speed-flow relationships has been slower due to the dearth of appropriate traffic data.

The calibration of speed-flow curves requires empirical data (average speed and flow rate disaggregated for passenger cars and heavy vehicles) for a representative sample of road segments. One of the byproducts of the Brazilian highway privatization program was the implementation of systematic traffic data collection, by means of a large number of permanent traffic-counting stations. The research reported in this paper was possible due to the availability of a large data set, collected at 24 traffic-counting stations on four major expressways in the state of São Paulo.

The main objectives of the research were to calibrate a family of speed-flow relationships for expressways in Brazil and to estimate capacity for these roads. This paper is organized such that initially, the mathematical modeling of the speed-flow relationship is discussed; next, the traffic data used is presented. Then the procedure used for the estimation of key parameters (density-at-capacity and the transition point) is presented, followed by the calibration of the speed-flow relationships and a comparison of the new curves with the HCM 2010 relationships.

2. MATHEMATICAL MODELING OF THE HCM SPEED-FLOW RELATIONSHIP

The mathematical model adopted to describe the speed-flow relationship in the HCM 2010 is the same one used in the HCM 2000 (*8*); furthermore, the same basic structure is used both for freeways and multilane highways. Assuming a traffic stream containing only passenger cars, this model comprises two regions (Figure 1.a): (I) a flat segment where traffic stream speed S is constant and equal to free flow speed (FFS); and (II) a convex segment, in which traffic stream speed varies between FFS and speed at capacity CS. The flow rate limits for the flat segment are 0 and BP, which is the transition point where traffic stream speed starts to decrease due to increase in flow rate. The convex segment limits are BP and capacity C.

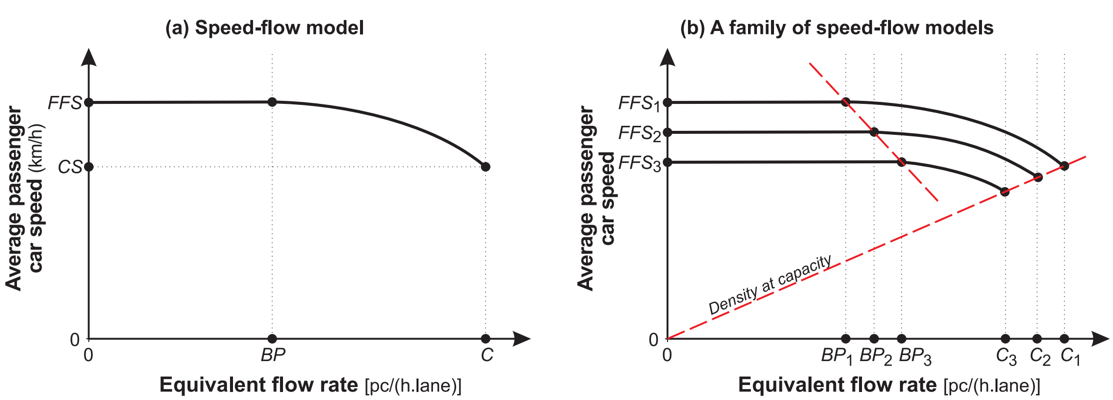

FIGURE 1 General characteristics of the HCM 2010 speed-flow model.

Empirical evidence from several studies supports this model (*9, 10, 11, 12, 13, 14*). The speed-flow function is "anchored" by two points: (BP, FFS) and (C, CS). The mathematical function $S = f(FFS, q)$ that represents the speed-flow model for freeways can be written as (*15*):

$$S = \begin{cases} FFS, \quad 0 \le q \le BP \\ FFS - \left[\frac{1}{28}(23FFS - 1800)\left(\frac{q + 15FFS - 3100}{20FFS - 1300} \right)^{2.6} \right], \quad BP < q \le C; \end{cases} \tag{1}$$

where S is traffic stream speed (km/h); q, traffic flow rate in pc/(h.lane); and FFS, BP and C are as previously defined. The HCM 2000 assumes density at capacity as 28 pc/(km.lane), a value that is hard-coded into Equation 1, but could be called CD.

Equation 1 can be used to create a family of speed-flow relationships for a set of free flow speeds $\{FFS_1, FFS_2, \ldots\}$ (Figure 1.b) using appropriate values of BP and C, which can be calculated using:

$$BP = -15FFS + 3100; \text{ and} \tag{2}$$

$$C = 5FFS + 1800. \tag{3}$$

Equation 2 shows that BP decreases linearly with increases in FFS. Equation 3 assumes that density at capacity remains constant and is equal to 28 pc/(km.lane) for any FFS.

By substituting Equations 2 and 3 into Equation 1 and making $CD = 28$ pc/(km.lane) and $\gamma = 2.6$, the relationship between S and C, CD, BP and FFS becomes:

$$S = FFS - \left(FFS - \frac{C}{CD} \right) \cdot \left(\frac{q - BP}{C - BP} \right)^{\gamma}. \tag{4}$$

Assuming that $C = CS \cdot CD$ and thus, $CD = C/CS$, Equation 4 can be simplified into:

$$S = FFS - \left[\left(FFS - CS \right) \frac{(q - BP)^{\gamma}}{(C - BP)^{\gamma}} \right]. \tag{5}$$

Equations 2 and 3 can also be generalized, as they imply that BP and C vary linearly with FFS. Therefore, these functions are:

$$BP = a_{BP} FFS + b_{BP}; \text{ and} \tag{6}$$

$$C = a_C FFS + b_C, \tag{7}$$

in which a_{BP}, b_{BP}, a_C and b_C are calibration constants.

Equations 5, 6, and 7 specify a generalized speed-flow model for freeways and divided multilane highways, from which the HCM 2010 relationships can be obtained. The next sections in this paper show how a set of speed-flow relationships was obtained for Brazilian expressways, by finding appropriate values for the parameters in these three equations.

3. SPEED-FLOW DATA FROM TRAFFIC SENSORS

Data for the calibration of the speed-flow relationship should ideally originate from streams containing only passenger cars and should also reflect normal operating conditions for uncongested flows (*16*).

Data used in this study were collected at 24 traffic-counting stations in the metropolitan region of São Paulo, using inductive loops installed in each traffic lane. The data were collected between 1/1/2010 and 8/31/2011 and consisted of number of vehicles (passenger cars and heavy vehicles) and average speed (for passenger cars and for heavy vehicles). For 11 of the 24 sites, data were available for 6-minute intervals; for the others, for 5-minute intervals. The HCM 2010 used 15-minute data points (*8*); several other studies, however, recommend the use of a 5-minute interval (*17, 18, 19*), which is deemed suitably short to represent the traffic behavior in greater detail and sufficiently long to avoid the introduction of bias in the estimation of speed and flow due to the inherent variability of driver behavior.

The process used for choosing sites for the sample is described in detail elsewhere (*20*). All segments in the sample meet conditions necessary to warrant uninterrupted flow, such as the existence of a physical median, no traffic signals and no ramps at least 3 km away from the site. According to the HCM, all sites in the sample could be classified either as *freeways* (expressways with controlled access) or as *divided multilane highways* (expressways without controlled access). Lane width (3.5 m) and left and right shoulder widths (respectively 0.6 m and 2.5 m) were constant across all segments, which contained at least three lanes in each direction (except two sites on SP270, with two lanes in each direction).

Sites in the sample were also classified as "rural" or "urban", according to abutting land use. "Rural expressways" comprised highways isolated from the local road network, bearing mostly longer trips; "urban expressways" are those with greater integration with the local network, with greater density of ramps and/or points of access, within an urbanized environment and carrying a significant portion of local trips. For each site in the sample, *FFS* was estimated to the nearest km/h, varying between 78 and 130 km/h. Speed-flow data indicate that capacity is often reached in 8 of the 24 sites.

There are two major differences between traffic streams in Brazil and in the U.S.A.: Brazil has a higher percentage of trucks in the flow; and mass-to-power ratios are greater in Brazilian trucks, when compared to American trucks. Furthermore, the practice in Brazil is to have two speed limits: a greater one (up to 120 km/h) for light vehicles (passenger cars) and a lower one (90 km/h) for heavy vehicles (trucks and buses). On expressways with three or more lanes, trucks and buses are not allowed to travel on the leftmost lane (closest to the median). The combined effect of this rule and poor performance characteristics is that trucks tend to stay on the right lanes (closest to the shoulder), while cars mostly travel on the left lanes, creating something similar to two fluids flowing with different speeds within the same stream. Speed-flow data show that the percentage of heavy vehicle in the flow is typically very low (usually less than 5%) on the leftmost lane, on which peak flow rates are greater than 2100 veh/(h.lane). On the rightmost lane, trucks comprise about 45% of the flow and the greatest flow rates observed barely reach 1500 veh/(h.lane). On the center lane, where truck percentages are between these two extremes (usually around 20%), an intermediate behavior was observed: the greatest flow rates observed were between 1500 and 1800 veh/(h.lane).

In order to use speed-flow data closest to base conditions, only data collected by the sensors on the leftmost lane of each site were used. Speed-flow data collected under bad weather conditions (rain) were also discarded from the sample. Additionally, observations with $P_T > 5\%$ were discarded; data points with $0 < P_T \leq 5\%$ were used, to avoid excessive thinning of the data set, especially in the region closer to capacity. For these cases, however, heavy vehicles were converted into passenger car equivalents (pce) using equivalence factors derived for these expressways in another study (*7*). After this selection, 788,122 observations, for the 24 sites, were available for use.

Initially, the data were divided into four groups: freeways (rural and urban) and divided multilane highways (rural and urban). The major factors used to classify each site were access control and surrounding land use. A visual inspection of these data sets, however, suggested that the differences between rural and urban sites were much stronger than the differences due to road type (freeway vs. multilane highways), as graphs in Figure 2 illustrate. Data point colors in Figure 2 indicate the number of observations for given speed-flow combinations, as shown in the legend.

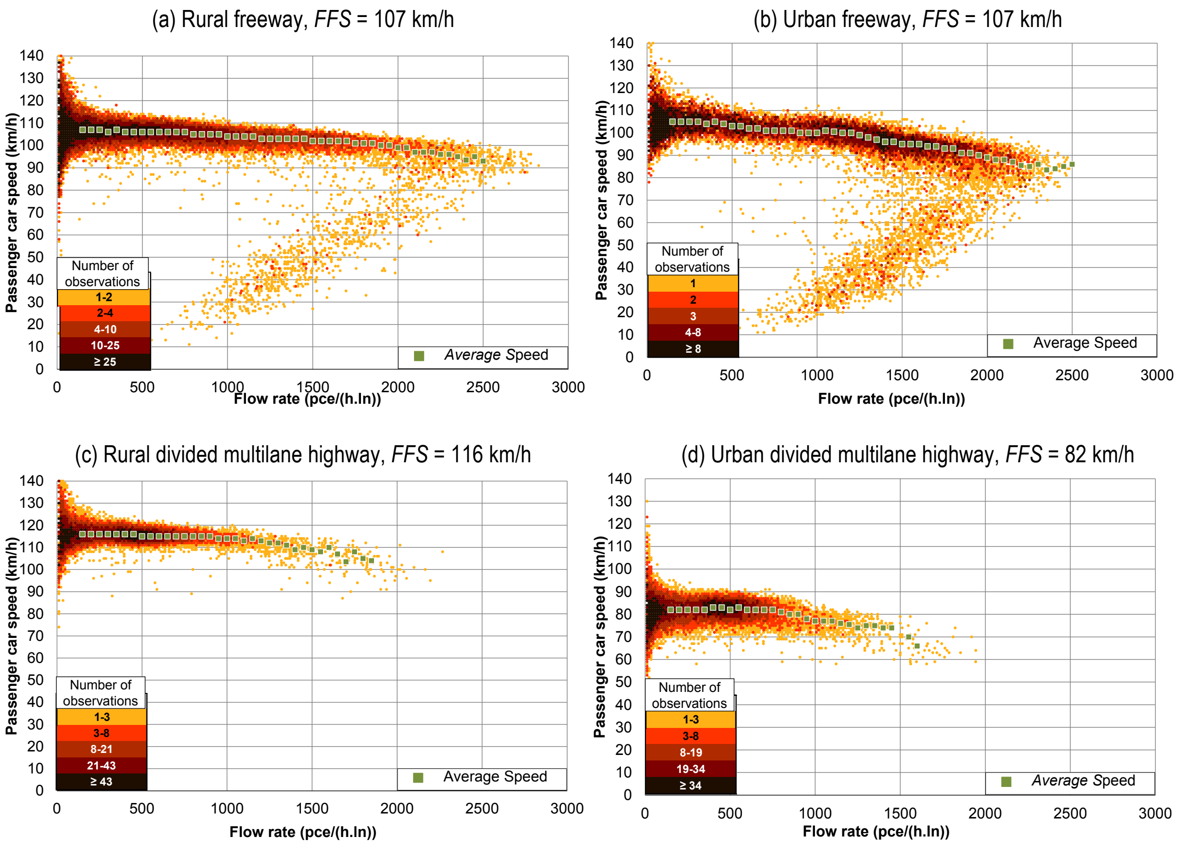

FIGURE 2 Speed-flow data for rural and urban expressway segments.

The graphs in Figure 2.a and 2.b show data collected on a rural freeway segment and an urban freeway segment with similar characteristics. Average traffic speeds are nearly constant over a greater range of flow rates in the rural segment, when compared to the urban segment. Also, average speed appears to decrease at a greater rate in the urban segment, when compared to the rural freeway section. Speed-flow data collected at rural divided multilane highways exhibit characteristics closer to those of rural freeways than those collected at urban divided multilane highway segments, as Figures 2.c and 2.d illustrate. Capacity for urban segments seems to be smaller than for rural segments and the speed-at-capacity is also smaller for urban expressways. Therefore, it was decided that the speed-flow models should be calibrated for rural and urban expressways, instead of the freeway vs. multilane highway approach used in the HCM.

4. ESTIMATION OF DENSITY AT CAPACITY FOR BRAZILIAN EXPRESSWAYS

While capacity is stochastic by nature (*21*), the speed-flow model shown in Figure 1 and in

Equations 5, 6 and 7 requires the estimation of deterministic values for capacity (*C*), free-flow speed (*FFS*), density at capacity (*CD*) and the traffic stream breakdown flow (*BP*). This section describes the procedure adopted to estimate density at capacity, which was adapted from the literature (*19, 22*).

4.1. Traffic stream breakdown and the definition of capacity

Breakdown in an uninterrupted traffic stream may be defined as the transition between proper operation and unacceptable flow conditions (*22*) and corresponds to a sudden reduction in average travel speed, reflecting the change from uncongested to congested flow. Recent studies (*19, 21, 22*) have suggested using breakdown flows to define the capacity of an expressway lane. This definition of capacity ("the volume below which the facility conditions are acceptable and above which the facility condition becomes unacceptable") is stochastic by nature (*21*).

The approach used to estimate capacity via traffic breakdown events is based on the Product Limit Method (PLM) and on an analogy with lifetime data analysis (*23*). The method assumes that the capacity distribution function is (*19*):

$$F_c(q) = p(c \le q)\,, \tag{8}$$

in which $F_c(q)$ is the capacity distribution function, *c* is capacity and *q* is the traffic flow rate. Using an analogy to lifetime data analysis, capacity *c* is analogous to the lifetime *T* of a technical component. The lifetime distribution function is:

$$F(t) = p(T \le t) = 1 - S(t)\,, \tag{9}$$

where $F(t)$ = distribution function of lifetime, that is, the probability that lifetime $T \le t$; and $S(t)$ is the survival function, that is, the probability that the lifetime $T > t$.

The PLM can be used to estimate the survival function using the expression (*19*):

$$\hat{S}(t) = 1 - \prod_{j:t_j<t} \frac{n_j - d_j}{n_j}, \tag{10}$$

where $\hat{S}(t) =$ the estimated survival function; $n_j =$ number of individuals with a lifetime $T \ge t_j$; and $d_j =$ number of deaths at time t_j. Each observed lifetime is used as one t_j value and, thus, $d_j = 1$ in Eq. 10.

Assuming that $\hat{S}(t) = S(t)$, the distribution function for the capacity analysis can be rewritten as

$$F_c(q) = 1 - \prod_{i:q_i \le q} \frac{k_i - d_i}{k_i}; \quad i \in \{B\}, \tag{11}$$

where
- $F_c(q)$: distribution function of capacity *c*;
- q: traffic flow rate (pc/h);
- q_i: traffic flow rate during interval *i* (pc/h);
- k_i: number of intervals in which $q \ge q_i$;
- d_i: number of breakdowns at a flow rate of q_i; and
- $\{B\}$: set of breakdown intervals.

To use Eq. 11, observations of average speed and traffic flow rates during short intervals are required, usually 5-minute intervals (*19, 21, 22*). The available speed-flow observations are arranged chronologically and classified into one of the following sets:

- $\{F\}$: traffic is uncongested in time interval i and also in time interval $i+1$, suggesting that flow rate q_i is not greater than capacity;
- $\{B\}$: traffic is uncongested in time interval i, but the observed flow rate in time interval $i+1$, q_i, causes the average speed to drop below a threshold, indicating that a breakdown occurs in time interval $i+1$; and
- $\{C\}$: traffic is congested in time interval i, either in the segment under consideration or spilling back from a downstream location – i.e., the average speed is below the threshold value. This time interval does not provide information about the capacity value and these flow rates are not used in the analysis.

Once the traffic flow observations are classified into these sets, the distribution function $F_c(q)$ can be plotted for flow rate values in $\{B\}$ set. A more detailed description of this procedure can be found in (*19*).

4.2. Definition of speed threshold values to identify breakdowns

The key to identifying a breakdown event is, therefore, a sudden drop (below a predefined threshold) in average speed during the next time interval. Previous researchers have adopted deterministic values for this threshold. In a study using data from freeways in Canada a threshold of 90 km/h was adopted (*24*); another study, using data from German freeways, adopted a threshold of 70 km/h, but stressed that other locations would likely produce different values (*22*).

Given the stochastic character of the breakdown event pointed out in the literature (*19, 22, 24*), in this study a statistical approach was used to find the threshold, assuming that the speed that marks the transition from the uncongested to congested conditions could be different for each site in the sample. The threshold value was determined using cluster analysis. The *k*-means method was used with the Euclidian distance as the distance metric (*25*). For each of the eight sites where capacity was reached, speed-flow observations for flow rates greater than 1750 pce/(h.lane) were classified into two clusters (uncongested and congested flow). The threshold is the speed that is simultaneously the lowest speed value for observations belonging to the uncongested flow regime and the highest speed for observations in the congested regime. Threshold values varied between 75 and 90 km/h, with an average of 83.3 km/h and a median of 83.5 km/h. *FFS* for these sites ranged from 105 to 116 km/h, with an average of 109 km/h and a median of 107 km/h; speed limits for passenger cars were 100, 110 or 120 km/h, depending on the site.

4.3. Estimation of capacity

Once all observations were classified into the appropriate sets, the survival function could be estimated, using the PLM. The maximum value of the distribution function of capacity only reaches 1 if the highest flow rate in the sample belongs to the $\{B\}$ set. In this case, the product in Eq. 11 will be zero and $F_c(q)=1$; otherwise $F_c(q)<1$. When the highest observed flow rate does not provoke a breakdown in the next time interval, it is impossible to estimate the complete capacity distribution function and some assumption about the mathematical type of $F_c(q)$ must be made (*19*). As in previous studies (*19, 21, 22*), the Weibull distribution was used in this research.

Capacity, under this approach, is not a deterministic value, but a random variable, following a statistical distribution. Should a capacity value be required, it can be estimated assuming a breakdown probability value under $F_c(q)$. The estimate for capacity is obtained from the flow rate associated with this breakdown probability through the speed-flow curve, as shown in Figure 3. The horizontal axis shows flow rates; the left vertical axis represents the average speed; the right *y*-axis shows the breakdown probability associated with the PLM model (red dots) and the fitted Weibull distribution (black line). Once a suitable value for the breakdown probability is chosen, the corresponding flow rate, which represents capacity, is found from the Weibull distribution function (dotted line).

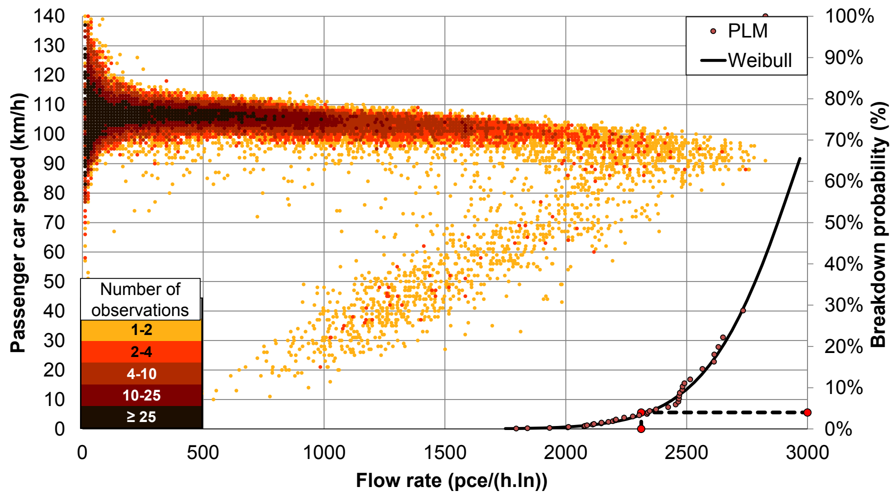

FIGURE 3 Speed-flow data, PLM model and fitted Weibull distribution for site SP021, km 22 N.

The value for the acceptable breakdown probability is key to the estimation of capacity. Geistefeldt (*26*) suggested $p = 3\%$ (i.e., the 3rd percentile of the fitted Weibull distribution); Washburn *et al*. (*19*) suggested using the 4th percentile. In this study, the value adopted was $p = 4\%$.

Once capacity *C* is known, density at capacity *CD* can be calculated using $CD = C/CS$. Speed at capacity *CS*, for this study, was assumed to be the average of all observations for flow rate *C* in the uncongested flow regime.

4.4. Results for estimation of density at capacity

The procedure was applied to the eight sites where capacity was reached. Figure 3 shows data collected at km 22 N on SP021. Capacity is 2250 pc/(h.lane) and the average traffic speed at capacity is 88 km/h; thus density at capacity is $2250/88 = 25.6$ pc/(km.lane). Table 1 summarizes the results.

TABLE 1 Capacity, speed at capacity and density at capacity estimates for the sample

Location	Land use	*FFS* (km/h)	*C* (pc/h.lane)	*CS* (km/h)	*CD* (pc/km.lane)	*Grade* (%)
SP348 km 32 N	Rural	116	2400	93	25.8	3.5%
SP021 km 18 N	Rural	108	2390	90	26.5	-1.0%
SP021 km 18 S	Rural	105	2375	87	27.3	1.0%
SP021 km 22 N	Rural	107	2312	95	24.3	-2.0%
SP280 km 27 E	Urban	107	2145	88	24.4	3.5%
SP280 km 29 E	Urban	105	2165	86	25.2	2.0%
SP280 km 37 E	Rural	116	1950	96	20.3	5.0%
SP280 km 51 E	Rural	110	1975	88	22.4	4.5%

The estimates for *CD* in Table 1 are very similar, except for two of the sites. These sites are steeper grades; thus an explanation for lower capacity could be the combined effects of grade magnitude and length. Therefore, these two sites were excluded from the sample, to avoid any bias in the estimation of *CD*. The average *CD* for urban sites is 25 pce/(km.lane) and the average *CD* for rural sites is 26 pce/(km.lane). The HCM 2010 adopts 28 pce/(km.lane) for freeways and 25 pce/(km.lane) for multilane highways.

5. TRANSITION POINT *BP*

The other key point that defines the speed-flow function is *BP*, the transition point between the flat and the curved portions of the functions (see Figure 1). The estimation of values for *BP* was based on the method used in the HCM 2010 (*8*). In the development of the HCM 2010, the data set used for the calibration of the functions was built by clustering all speed-flow observations for sites with similar *FFS*. However, Roess (*8*) argues that the results were unsatisfactory, from a regression statistics viewpoint, and required judgmental adjustments. A slightly different approach was used: *BP* was estimated for each site and this set of *BP* values was used to fit a *BP* function.

5.1. Method

Assuming that in the first portion of the speed-flow relationship, the average speed is equal to *FFS*, one can calculate the standard deviation σ of the observed speeds x_i with relation to *FFS*:

$$\sigma = \sqrt{\frac{\sum\left(x_i - FFS\right)^2}{N}}\ , \qquad (12)$$

where x_i is the observed speeds for a given range of traffic flows (e.g., 200–250 pc/h.lane); *N* is the number of speed observations for that flow range; and *FFS* is the free flow speed for the site. To find *BP*, Roess (2011) plotted σ vs. flow rate; *BP* corresponds to the minimum value of σ. In this study, a third-degree polynomial was fitted to the function $\sigma = f(q)$ and *BP* was defined as the flow rate for which the derivative of the fitted polynomial becomes positive – corresponding to the point at which σ starts to increase. The third-degree polynomial was chosen because it provided the best fit to the data. Also, this procedure can be automated in an Excel spreadsheet and provides a criterion for selecting *BP* that does not depend on judgment.

5.2. Results for estimation of break points

The method was applied to all sites in the sample because the transition point can be found even for sites that do not reach capacity. For each site, σ was calculated for each 50-pc/(h.lane) range for flows rates greater than 200 pc/(h.lane) (i.e., 200–250, 250–300 and so on). The graphs in Figure 4 illustrate the procedure.

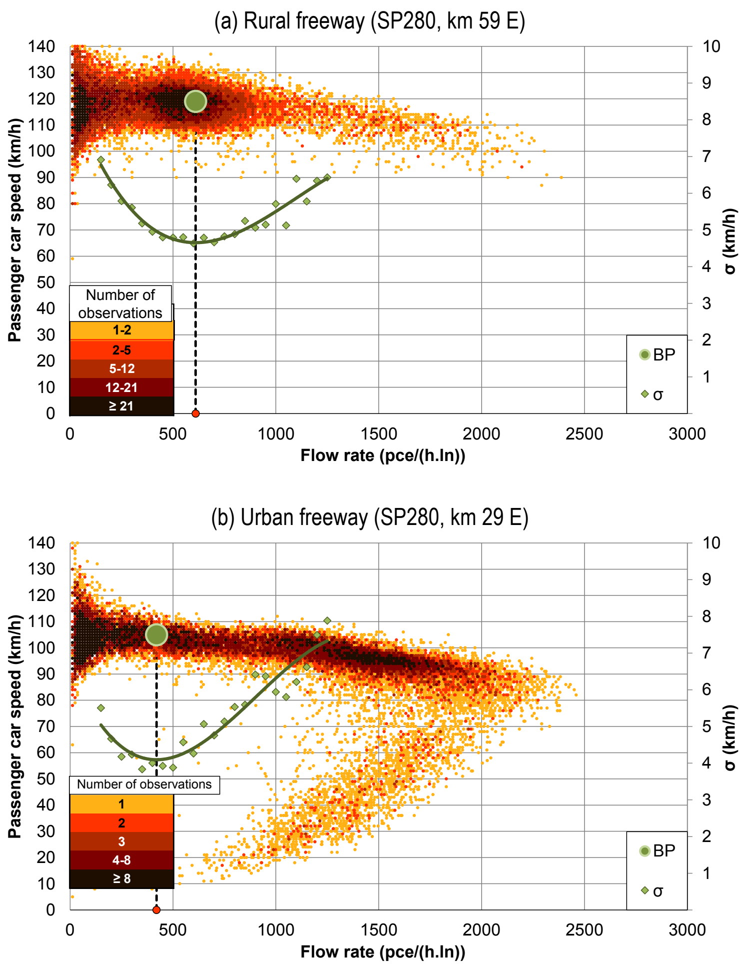

FIGURE 4 *BP* and the speed standard deviation around *FFS*, for two sites on SP280.

The left vertical axis on Figure 4 shows the speed and the right *y*-axis, the standard deviation for speeds around *FFS*. Speed-flow observations are orange-to-black points; green data points are σ vs. flow data; and the green curve is the fitted polynomial. The bigger green dot represents *BP* for the site (i.e., the minimum of the fitted polynomial). For the site shown in the graph of Figure 4.a, a rural location, *BP* is 530 pce/(h.lane); for the other site, an urban location, *BP* is estimated as 420 pce/(h.lane).

The results suggest that the vertical profile has little influence on *BP*, thus data from all sites could be used in the analysis. Note that *BP* decreases as *FFS* increases, and that the rate of decrease is greater for urban sites. The values for *BP* found for urban expressways were smaller than those found for rural expressways. The relationship between *BP* and *FFS*, for rural expressways, was

$$BP = -7.6\,FFS + 1422 \quad (R^2 = 0.53)\,; \tag{13}$$

and the model fitted for urban expressways was

$$BP = -3.75\,FFS + 835 \quad (R^2 = 0.62)\,. \tag{14}$$

In both cases, the values found for *BP* (in km/h) are significantly lower than those presented in the HCM 2010, evidencing the differences between American and Brazilian drivers. Whereas these differences undoubtedly exist, they might be smaller, since Roess has also found lower values for *BP*, which were later increased by the freeways committee to make the curves achieve a more uniform appearance (*8*).

6. SPEED-FLOW RELATIONSHIPS FOR EXPRESSWAYS IN BRAZIL

Once the "anchor" points for the convex segment of the speed-flow relationships were estimated, the next step was the calibration of the speed-flow functions. This calibration involves finding the best values for parameters used in Equations 5, 6 and 7; i.e., those values that minimize the differences between observed speed-flow data and speed-flow estimates obtained using the model. The adopted approach consisted in finding the calibration parameter set that minimized the error for all data collection locations simultaneously.

6.1. Data set for calibration and calibration procedure

To create the data set for calibration of the speed-flow functions, speed-flow observations for the 24 stations were divided into sets covering 50-pce/h ranges (i.e., 0–50 pce/h, 51–100 pce/h and so on). The median for speeds was then calculated for each set, for sets with at least 10 observations. Thus, a total of 957 points (average and median) were obtained, including 237 points for urban sites and 720 for rural sites. Figure 5.a illustrates the data, showing the median of observed speeds for three of the 24 sites in the sample.

The use of the median for each flow rate range, instead of the actual speed-flow observations was chosen to avoid bias due to greater density of information for lower flow rates, when compared to the number of observations closer to capacity (*18*). The adopted approach ensures two conditions: (1) each flow range has the same weight when calibrating the speed-flow function; and (2) the data from sites where capacity is reached have a greater influence on the calibrated function than data from sites where capacity is not reached.

The calibration procedure used involves an optimization problem whose objective is to minimize the squared error between the speed estimated using the model and the median of observed speeds for each of the 957 points in the sample, as used in other studies (*27, 28*).

Given that the "anchor points" *BP* and *CD* are fixed, there are three unknowns: the constants a_C and b_C in Equation 7, which defines capacity, and the exponent γ in Equation 5, which determines the "concavity" of the function. Furthermore, in order to produce a consistent set of curves (i.e., curves with similar shapes), the following restrictions were imposed: (1) $\gamma \geq 1$ and has the same value for any *FFS*, to ensure the same concavity and shape for all speed-flow curves; (2) *BP* must be constant or a function of *FFS* (as in Equations 13 and 14); and (3) *C* and *CS* must also be a function of *FFS*.

A non-linear optimization algorithm, the Generalized Reduced Gradient (GRG2) Algorithm, implemented in MS-Excel was used to solve the problem. To avoid local optima, the procedure was replicated 10 times, with different seeds, and the best solution was chosen.

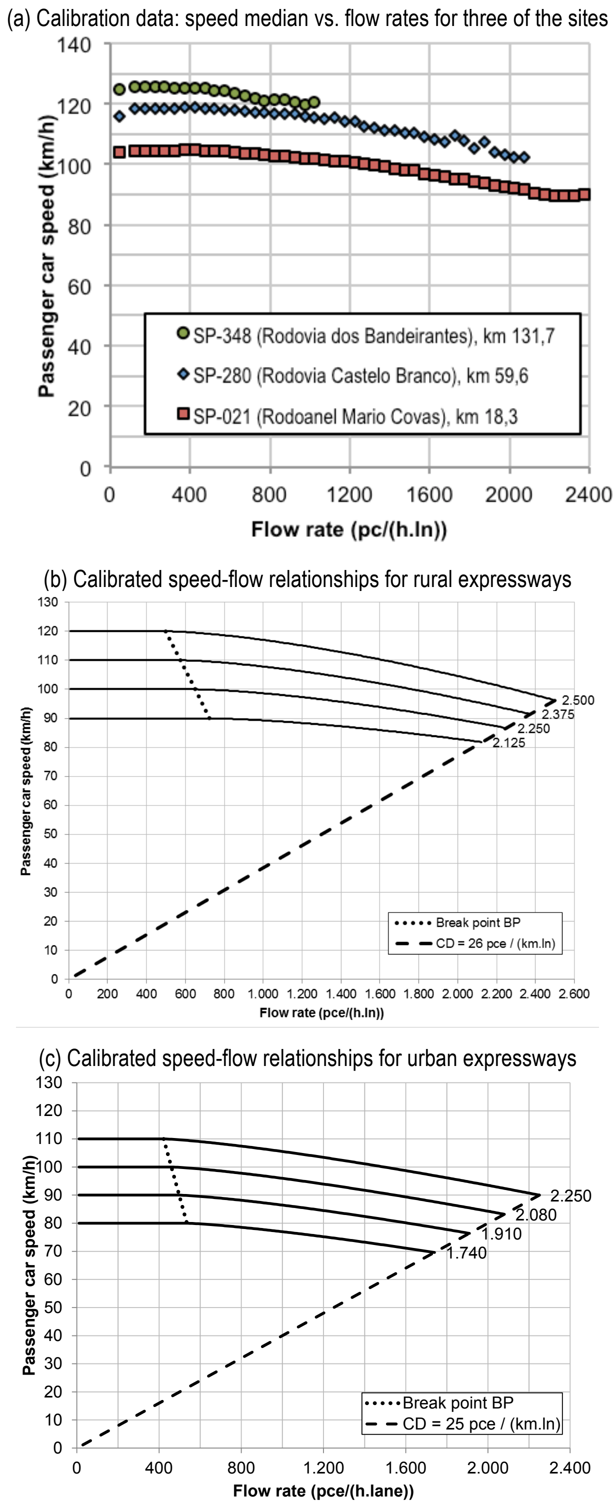

FIGURE 5 Proposed speed-flow relationships for expressways in Brazil: (a) data set for calibration of the models; (b) calibrated models for rural expressways; (c) calibrated models for urban expressways.

Figure 5.b exhibits the proposed speed-flow relationships for rural expressways. The

calibrated model is:

$$S = \begin{cases} FFS, & \text{if } v \le -7.5FFS + 1400 \\ FFS - \left(FFS - \dfrac{C}{26}\right)\left[\dfrac{v - (-7.5FFS + 1400)}{C - (-7.5FFS + 1400)}\right]^{1,5} & \end{cases} \quad (15)$$

with $C = 12.5FFS + 1000$,

where S is the traffic stream average speed (km/h); ν is the traffic flow rate (pc/h.lane); *FFS* is the *FFS* (km/h); and C is capacity (pc/h.lane). The dotted line in Figure 5.b shows *BP*, the limit for the flat portion of the speed-flow relationship; and the broken line in Figure Figure 5.b represents density at capacity (26 pc/km.lane).

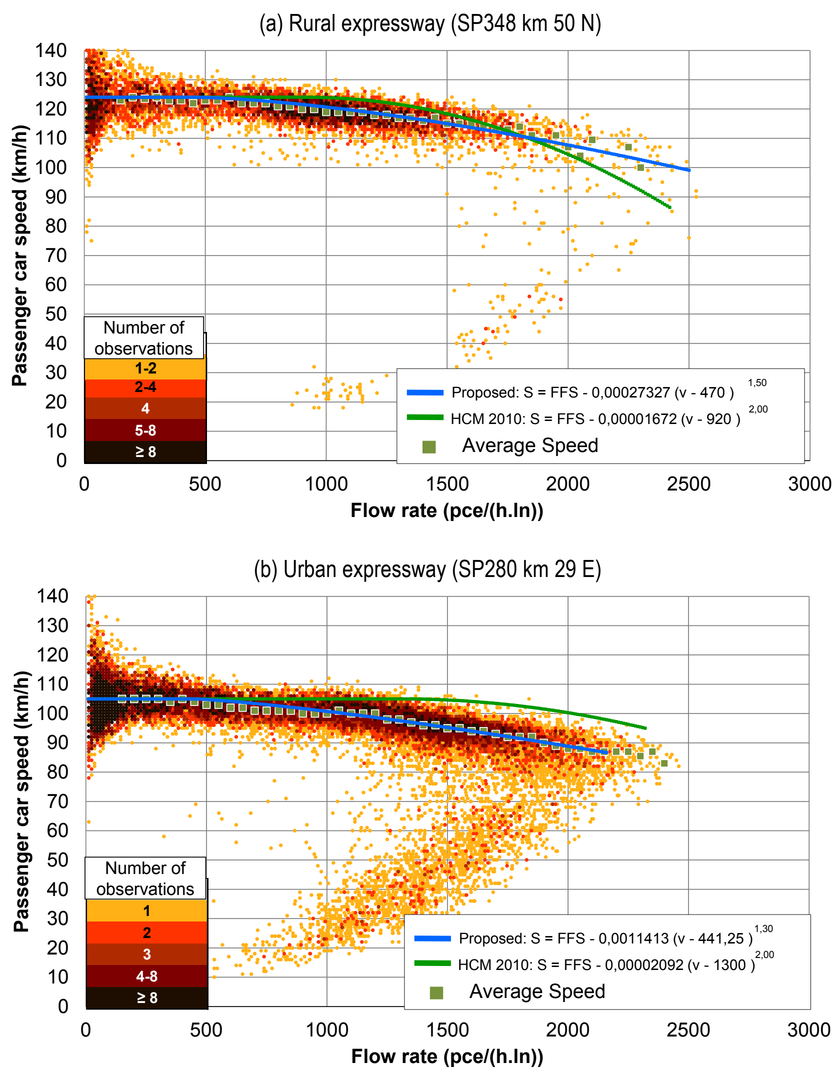

FIGURE 6 Comparison of speed-flow relationships (proposed model and HCM 2010 model) to empirical data for two sites in Brazil.

The graph in Figure 5.c shows the proposed speed-flow relationships for urban expressways, which can be written as:

$$S = \begin{cases} FFS, & \text{if } v \le -3.75FFS + 835 \\ FFS - \left(FFS - \dfrac{C}{25}\right)\left[\dfrac{v - (-3.75FFS + 835)}{C - (-3.75FFS + 835)}\right]^{1,3} \end{cases} \qquad (16)$$

with $C = 17FFS + 380.$

The transition point *BP* is represented by a dotted line in Figure 5.c and capacity at density, by a broken line. Note that, for urban expressways, the transition point *BP* appears at lower flow rates, compared to rural expressways. Furthermore, estimates of capacity *C* and speed at capacity *CS* are greater for rural expressways than for urban expressways.

The graphs in Figure 6 compare the HCM 2010 model for freeways (green line) to the proposed model (blue line) and the empirical speed-flow data, for a rural expressway and for an urban expressway. In both cases, the proposed models are clearly a better fit. The HCM 2010 models, which were calibrated using data from American freeways, overestimate the speed for flow rates between 1000 and 1800 pc/(h.lane) and underestimate the speed for flow rates greater than 2000 pc/(h.lane). Table 2 summarizes the comparison between the proposed models and the HCM 2010 models.

TABLE 2 Estimated values for main parameters of speed-flow relationships for rural and urban expressways in Brazil

	Transition point *BP* (pc/h.lane)		**Capacity *C*** (pc/h.lane)		**Speed at capacity *CS*** (km/h)	
FFS (km/h)	Proposed model	HCM 2010	Proposed model	HCM 2010	Proposed model	HCM 2010
Rural						
120	500	1000	2500	2400	96	86
110	575	1200	2375	2350	91	84
100	650	1400	2250	2300	87	82
90	725	1600	2125	2250	82	80
Urban						
110	420	na*	2250	na	90	na
100	460	na	2080	na	83	na
90	500	na	1910	na	76	na
80	535	na	1740	na	70	na

(*) n.a. = not applicable

7. CONCLUDING REMARKS

This paper presents a set of speed-flow relationships for expressways in Brazil developed to replace the original curves presented in the HCM 2010. The models are based on formulations adopted in the development of the HCM 2010 speed-flow curves and were calibrated using speed-flow data collected in 24 permanent traffic-counting stations in highways in the state of São Paulo. The empirical data showed that access control does not influence traffic behavior as much as abutting land use; therefore, the proposed models are divided into urban vs. rural instead of using the HCM 2010 freeways vs. multilane highways scheme. Compared to the HCM 2010 models, the proposed speed-flow relationships present: (1) lower density at capacity: 26 pc/(km.lane) for rural sites and 25 pc/(km.lane) for urban segments; (2) significantly lower break points *BP*, beyond which congestion starts to reduce the speed of the traffic stream; (3) higher speed at capacity; and (4) greater capacity for segments with higher *FFS* (120 and 110 km/h) and lower capacity for segments with lower *FFS* (100 and 90 km/h).

As expected, the proposed models were better fitted to the traffic data than the HCM 2010 models. However, it would be very desirable to increase the sample size, to include not just more sites, but especially sites with *FFS* around 90 km/h and segments in mountainous terrain, which were missing in the available sample. An extension of this research is currently under way to analyze traffic flows on a lane-by-lane basis, given the observed differences in truck percentages.

Acknowledgements

The authors thank the support from ARTESP, CCR RodoAnel, CCR ViaOeste and CCR AutoBan, which kindly provided traffic data. The authors also acknowledge the financial support provided by CNPq for this research (grant 303341/2008-4).

REFERENCES

1. DNIT. *Manual de Estudos de Tráfego*. Publication IPR-723. Departamento Nacional de Infraestrutura de Transportes, Instituto de Pesquisas Rodoviárias, Rio de Janeiro, Brazil, 2006.
2. Demarchi, S. H., and J. R. Setti. Limitations of passenger-car equivalent derivation for traffic streams with more than one truck type. In *Transportation Research Record: Journal of the Transportation Research Board, No. 1852*, Transportation Research Board of the National Academies, Washington, D.C., 2003, pp. 96–104.
3. Egami, C. Y., and J. R. Setti. Adaptação do HCM2000 para Determinação do Nível de Serviço em Rodovias de Pista Simples no Brasil. *Transportes*, Vol. 14, No. 2, 2006, pp. 27–34. http://revistatransportes.org.br/anpet/article/view/66. Accessed July 29, 2013.
4. Andrade, G. R., K.C. Rodrigues-Silva, and R. G. Gouvêa. Aplicabilidade das Metodologias Rodoviárias do Highway Capacity Manual 2000 no Brasil. In *Anais do XXII Congresso de Pesquisa e Ensino em Transportes – Fortaleza*. CD-ROM. Associação Nacional de Pesquisa e Ensino em Transportes, Rio de Janeiro, Brazil, 2008.
5. Setti, J. R. Highway Capacity Manual ou Manual de Capacidade Viária? In *Anais do 6° Congresso Brasileiro de Rodovias e Concessões – CBR&C 2009*. CD-ROM. Associação Brasileira de Concessionárias de Rodovias, Florianópolis, Brazil, 2009.
6. Andrade, G. R., K. C. Rodrigues-Silva and S. A. Puty-Filho. Panorama Normativo e Tecnológico da Avaliação Operacional das Concessões Rodoviárias. In *Anais do 7° Congresso Brasileiro de Rodovias e Concessões – CBR&C 2011*. CD-ROM. Associação Brasileira de Concessionárias de Rodovias, Foz do Iguaçu, Brazil, 2011.
7. Cunha, A. L., and J. R. Setti. Truck Equivalence Factors for Divided, Multilane Highways in Brazil. In *6th International Symposium on Highway Capacity and Quality of Service, 2011, Stockholm*. *Procedia – Social and Behavioral Sciences*. Elsevier, Amsterdam, Vol. 16, 2011, pp. 248–258.
8. Roess, R. P. Speed-Flow Curves for Freeways in the 2010 HCM. In *Transportation Research Record: Journal of the Transportation Research Board, No. 2257*, Transportation Research Board of the National Academies, Washington, D.C., 2011, pp. 10–21.
9. Hall, F. L. and K. Agyemang-Duah. Freeway Capacity Drop and the Definition of Capacity. In *Transportation Research Record: Journal of the Transportation Research Board, No. 1320*,

Transportation Research Board of the National Academies, Washington, D.C., 1991, pp. 91–98.

10. Urbanik II, T., W. Hinshaw, and K. Barnes. Evaluation of High-Volume Urban Texas Freeways. In *Transportation Research Record: Journal of the Transportation Research Board, No. 1320*, Transportation Research Board of the National Academies, Washington, D.C., 1991, pp. 110–118.
11. Banks, J. H. Flow Processes at Freeway Bottleneck. In *Transportation Research Record: Journal of the Transportation Research Board, No. 1287*, Transportation Research Board of the National Academies, Washington, D.C., 1990, pp. 20–28.
12. Persaud, B. N. and V. F. Hurdle. Some New Data that Challenge Some Old Ideas About Speed-Flow Relationships. In *Transportation Research Record: Journal of the Transportation Research Board, No. 1194*, Transportation Research Board of the National Academies, Washington, D.C., 1988, pp. 191–198.
13. Hall, F. L. and L. M. Hall. Capacity and Speed-Flow Analysis of Queen Elizabeth Way in Ontario. In *Transportation Research Record: Journal of the Transportation Research Board, No. 1287*, Transportation Research Board of the National Academies, Washington, D.C., 1990, pp. 20–28.
14. Chin, H. C., and A. D. May. Examination of the Speed-Flow Relationships at the Caldecott Tunnel. In *Transportation Research Record: Journal of the Transportation Research Board, No. 1320*, Transportation Research Board of the National Academies, Washington, D.C., 1991, pp. 75–82.
15. *Highway Capacity Manual 2000*. Transportation Research Board of the National Academies, Washington, D.C., 2000.
16. *Highway Capacity Manual*. Transportation Research Board of the National Academies, Washington, D.C., 2010.
17. Demarchi, S. H. and J. R. Setti. Calibração da curva fluxo-velocidade-densidade para rodovias de pista dupla brasileiras. In *Anais do XI Congresso Panamericano de Engenharia de Trânsito e Transportes – Gramado, Rio Grande do Sul*. Associação Nacional de Pesquisa e Ensino em Transportes, Rio de Janeiro, Brazil, 2000, pp. 131–144.
18. Bassan, S. and A. Polus. Meaning of Actual Capacity of Freeways and its Estimation. *Canadian Journal of Civil Engineering*, Vol. 37, 2010, pp. 77–87.
19. Washburn, S. S., Y. Yin, V. Modi, and A. Kulshrestha. *Investigation of Freeway Capacity, Part B: Freeway Capacity Estimation for Florida Freeways, Final Report*. Transportation Research Center, University of Florida, Tallahassee, FL, 2010.
20. Andrade, G. R., and J. R. Setti. Método para Caracterização e Classificação de Trechos Homogêneos Rodoviários. *Anais do 7° Congresso Brasileiro de Rodovias e Concessões – CBR&C 2011*. CD-ROM. Associação Brasileira de Concessionárias de Rodovias, Foz do Iguaçu, Brazil, 2011.
21. Brilon, W., J. Geistefeldt, and H. Zurlinden. Implementing the Concept of Reliability for Highway Capacity Analysis. In *Transportation Research Record: Journal of the Transportation Research Board, No. 2027*, Transportation Research Board of the National Academies, Washington, D.C., 2007, pp. 1–8.
22. Brilon, W., J. Geistefeldt, and M. Regler. Reliability of Freeway Traffic Flow: A Stochastic Concept of Capacity. In *Proceedings of the 16th International Symposium on Transportation and Traffic Theory*, College Park, Maryland, 2005, pp. 125–144.
23. Kaplan, E. L. and P. Meier. Nonparametric Estimation from Incomplete Observations.

Journal of the American Statistical Association, Vol. 53, 1958, pp. 457–481.

24. Lorenz, M. and L. Elefteriadou. A Probabilistic Approach to Defining Freeway Capacity and Breakdown. In *Proceedings of the 4th International Symposium on Highway Capacity, Circular E-C018*. Transportation Research Board of the National Academies, Washington, D.C., 2001.
25. Bessa Jr., J. E., and J. R. Setti. Derivation of ATS and PTSF Functions for Two-lane, Rural Highways in Brazil. In *6th International Symposium on Highway Capacity and Quality of Service, 2011, Stockholm*. *Procedia – Social and Behavioral Sciences*. Elsevier, Amsterdam, Vol. 16, 2011, pp. 282–292.
26. Geistefeldt, J. Empirical Relation Between Stochastic Capacities and Capacities Obtained from the Speed-flow Diagram. In *75 Years of the Fundamental Diagram for Traffic Flow Theory – Greenshields Symposium*. Transportation Research Circular E-C149. Transportation Research Board of the National Academies, Washington, D.C., 2011, pp. 1–12.
27. Rakha, H. and M. Arafeh. Calibrating Steady-State Traffic Stream and Car-Following Models Using Loop Detector Data. *Transportation Science*, Vol. 44, No. 2, 2010, pp. 151–168.
28. Sun, L., J. Yang, H. Mahmassani, W. Gu, and B. J. Kim. Data Mining-Based Adaptive Regression for Developing Equilibrium Speed-Density Relationships. *Canadian Journal of Civil Engineering*, Vol. 37, 2010, pp. 389–400.